IEEE P802.11
Wireless LANs

Performance of the Proposed 2.4-GHz PHY

Date: May 1, 1998

Author: John H. Cafarella
MICRILOR, Inc.
17 Lakeside Office Park, Wakefield, MA 01880
Phone: 781-246-0103
Fax: 781-246-0157
e-Mail: JohnCafarella@worldnet.att.net

Abstract

This is a revised draft documenting the performance of the MICRILOR 2.4-GHz proposal.

1 Performance Summary

1.1 Implementation

RF/IF ≈ PRISM® chipset with PA replaced by lower power unit

Baseband chip ≈ 25K gates modem function + 10K gates control
+ Interoperability 8K gates

Diversity requires alternate antenna and incurs switch loss.

1.2 Immunity to Multipath and Noise

1.1.1 Without Diversity

Multipath Only
Using the 802.11-mandated Diffuse Rayleigh Multipath model, incorporation of a Channel Matched Filter (CMF), as dictated by maximum-likelihood processing applied to the diffuse multipath channel, extends the delay-spread tolerance to 275 ns for 10% PER (insensitive to packet length). The proposal is based upon inclusion of the CMF.

Noise Only
The Gaussian Channel performance: 10% PER for 1000-byte packet at an input SNR of 1.7 dB.

Noise and Multipath
At 275 ns delay spread, a 1000-byte packet experiences 20% PER at input SNR of 21.4 dB. At 150 ns a 1000-byte packet experiences 10% PER at an input SNR of 20.6 dB.

1.1.2 With Diversity

Gains approximately 1 to 2 dB reduction in required SNR.

1.2 Overhead Related Parameters

PLCP Preamble & Header: < 24 μs (with antenna diversity)

Slot size: 10 μs (with antenna diversity)

SIFS could be short, depending upon processor. Drop-down FEC mode incurs 7.5-μs latency, but end of reception can be timed from that point.

1.3 Spectral Efficiency and Cell Density Related Parameters

Channelization:

Frequency	Code

Two 10-Mbps frequency channels
One 10-Mbps + one 5-Mbps channel
One 10-Mbls + one 2-Mbps channel
Three channels, any mix of 2 & 5 Mbps
Three 1-/2-Mbps + 1 10-Mbps

`Eight search-code channels`

48 cyclic data code channels
64K pseudorandom data code channels

Cell Planning: BSAs operated with substantial spatial overlap of user areas if on different frequency channels; BSAs on same frequency channel is reasonable separation; always separate code channels as a matter of practice. Mix of 2-Mbps with 10-/5-Mbps channels. **It is possible to operate three legacy 1-/2-Mbps channels independently, and also operate a 10-Mbps high-rate channel on top of, and interoperating with, the middle legacy channel.**

Adjacent channel interference: On same frequency channel (CCI) , desired signal must exceed interfering signal by ≈ 2 dB. For different frequency channels (ACI) there is extra 35 dB isolation (as in low-rate standard).

Interference Immunity
>14-dB processing gain against CW
12-dB processing gain against >25% BW Gaussian noise

1.4 Critical Points

- Phase noise not an issue (non-coherent receiver)
- Power consumption very attractive (PA efficienty; E_B/N_0)
- Complexity not an issue (35K to 43K gates)
- RF PA backoff not required (MSK spreading modulation)
- Antenna diversity included

1.5 Intellectual Property

Letter to IEEE. Patent number not yet available. Will comply with IEEE guidelines. Call Dr. Stanley Reible.

1.6 Interoperability/Coexistence

Enhanced CCA possible for non-cooperative coexistence techniques described in D_97/128. Recommended coexistence based upon high-rate deferral when required.

Interoperability with 1-/2-Mbps DSSS via CCA matched filter. Dual-preamble not required; chip can process both; coordination via RTS/CTS exchange.

2 Multipath Models

2.1 Diffuse Rayleigh Channel

The Diffuse Rayleigh path model assumes that the channel impulse response comprises Rayleigh-distributed paths at discrete, uniformly spaced delays, filled in delay

$$h_c(t) = \sum_{k=0}^{\infty} a_k \delta(t - k\tau_s)$$

where τ_s is the delay spacing, and a_k is a complex amplitude whose real and imaginary components are Gaussian-distributed, with the following equivalent distributions:

$$p(\mathrm{Re}\{a_k\}) = \frac{1}{\sqrt{2\pi}\sigma_{ak}} e^{-\frac{\mathrm{Re}\{a_k\}^2}{2\sigma_{ak}^2}}$$

$$p(\mathrm{Im}\{a_k\}) = \frac{1}{\sqrt{2\pi}\sigma_{ak}} e^{-\frac{\mathrm{Im}\{a_k\}^2}{2\sigma_{ak}^2}}$$

real/imaginary components

$$p(|a_k|) = \frac{|a_k|}{\sigma_{ak}^2} e^{-\frac{|a_k|^2}{2\sigma_{ak}^2}}$$

$$p(Arg\{a_k\}) = \frac{1}{2\pi}$$

magnitude & phase

The path strengths are exponentially distributed in amplitude vs. delay

$$\sigma_{ak}^2 = \sigma_0^2 e^{-\frac{k\tau_s}{T_{RMS}}} \quad \text{with} \quad \sigma_0^2 = \frac{1 - e^{-\frac{\tau_s}{T_{RMS}}}}{2}$$

where T_{RMS} is the multipath RMS delay spread. The normalization of the path strengths holds the total received signal power constant as other parameters are varied. The multipath-delay spacing is the shorter of the spread-spectrum chip time T_c or half the delay spread T_{RMS}.

2.2 Other Channel Models

The Diffuse Rayleigh channel represents an extreme of channel behavior which stresses receiver design. For example, when the multipath is of more specular nature, then excellent performance can be achieved using a relatively simple receiver structure. Other channels have been proposed in the literature, but the 802.11 committee has not been able to agree on alternates. As a result, data for only the Diffuse Rayleigh channel is presented herein.

3 Signal Model

The transmit waveform[1] has the baseband representation

$$s(t) = \sum_m \sum_{n=0}^{M-1} j^n C_{mn} p_T(t-(n+mM)T_c)$$

where

T_c is the inverse of the chip frequency,
n is the chip index within a symbol,
M is the number of chips per symbol,
m is the symbol index,
C_{mn} is the chip code, and
$p_T(t)$ is the single-chip waveform:

During the acquisition preamble the chip value is

$$C_{mn} = C_{Sn}$$

where

C_{Sn} is the search PN code, $0 \le n < M-1$.

In the data portion of a frame the chip value is

$$C_{mn} = d_m P_{mn} W_{K_m n}$$

where

d_m is the polarity specified by the DBPSK component of the 16-ary DBOK signaling,
P_{mn} is the PN code during the m^{th} symbol,
W_{Kmn} is the Walsh function during the m^{th} symbol, and
K_m is specified by the 16-ary OK signaling component.

When transmitted, s(t) is convolved with the channel impulse response to yield the received waveform

$$r(t) = \sum_{k=0}^{\infty} a_k \sum_m \sum_{n=0}^{M-1} j^n C_{mn} p_T(t-kT_s-(n+mM)T_c)$$

At the receiver complex Gaussian noise z(t) is added, which obeys

$$\overline{z(t)} = 0$$

$$\overline{z(t)z(t')} = 0$$

$$\overline{z(t)^* z(t')} = 2N_0 \delta(t-t')$$

where N_0 is the one-sided noise spectral density. The waveform is then convolved with the aggregate receive filter to form x(t)=w(t)+q(t). The deterministic part w(t) (i.e., r(t) filtered) is

$$r(t) = \sum_{k=0}^{\infty} a_k \sum_m \sum_{n=0}^{M-1} j^n C_{mn} p_R(t-kT_s-(n+mM)T_c)$$

where $p_R(t)$ is the chip-pulse waveform after receive filtering.
The noise component q(t) (i.e., z(t) filtered) has variance

$$\overline{|q(t)|^2} = \sigma_N^2 = 2N_0 B_N$$

where B_N is the noise bandwidth of the receiver.

The filtered receive waveform is sampled at the chip rate to produce the sequence $x_n=w_n+q_n$.

$$w_n = r(t_0+nT_c) = \sum_{k=0}^{\infty} a_k \sum_m \sum_{n'=0}^{M-1} j^{n'} C_{mn'} p_R(t_0+nT_c-kT_s-(n'+mM)T_c)$$

[1] See Appendix on MSK Approximation.

The statistics of samples of the noise q_n will be the same as q(t). During acquisition the strongest path (at some delay $k_0\tau_s$) is selected for demodulation. We explicitly define the sampling time reference to correspond to the correct sampling time for the first chip of symbol m_0 on this strongest signal component; that is, we select $t_0=k_0\tau_s+m_0MT_c$. Thus, the signal sequence is

$$w_n = \sum_{k=0}^{\infty} a_k \sum_m \sum_{n'=0}^{M-1} j^{n'} C_{mn'} p_R((k_0-k)t_s + (n-n'+(m_0-m)M)T_c)$$

The correlator reference sample sequence is $j^{-n}B_{m_0n}$;[2] the correlator output is

$$Y_{Bm_0} = \sum_{n=0}^{M-1} j^{-l} B_{m_0n} w_n = \sum_{k=0}^{\infty} a_k \sum_m \sum_{n'=0}^{M-1} \sum_{n=0}^{M-1} j^{n'-n} B_{m_0n} C_{mn'} p_R((k_0-k)t_s + (n-n'+(m_0-m)M)T_c)$$

A number of chip values can contribute to the n^{th} sample because of the width of $p_R(t)$ and also because of the multipath delay spread. It is most natural to measure the delay spread in multiples, or sub-multiples, of the chip time because it simplifies analysis and simulations. For 0 delay spread we have a Gaussian channel; when the delay spread is a single chip time, then it is necessary to half-chip sampling of the multipath profile; for integer multiples greater than 1 the multipath profile is sampled at the chip time. The multipath will thus be sampled at T_c or ½T_c; the possible sampled values of $p_R(t)$ are[3]

$$p_{R0} = p_R(0) = 1$$

$$p_{R\frac{1}{2}} = p_R(\frac{T_c}{2}) = p_R(-\frac{T_c}{2})$$

$$p_{R1} = p_R(T_c) = p_R(-T_c)$$

Samples at $1.5T_c$ or greater from the time of the peak are approximately zero. We can make the replacement

$$p_R((k_0-k)t_s + (n-n'+(m_0-m)M)T_c) = \delta_{n-n'-(m_0-m)M+(k_0-k)\frac{t_s}{T_c}}$$

$$+ p_{R\frac{1}{2}}\left[\delta_{n-n'-(m_0-m)M+(k_0-k)\frac{t_s}{T_c}+\frac{1}{2}} + \delta_{n-n'-(m_0-m)M+(k_0-k)\frac{t_s}{T_c}-\frac{1}{2}}\right] + p_{R1}\left[\delta_{n-n'-(m_0-m)M+(k_0-k)\frac{t_s}{T_c}+1} + \delta_{n-n'-(m_0-m)M+(k_0-k)\frac{t_s}{T_c}-1}\right]$$

where the function[4] δ_x=1 if the index equals 0, and δ_x=0 otherwise).

$$Y_{Bm_0} = \sum_{k=0}^{\infty} a_k \sum_m \sum_{n'=0}^{M-1} \sum_{n=0}^{M-1} j^{n'-n} B_{m_0n} C_{mn'} \delta_{n-n'+(m_0-m)M+(k_0-k)\frac{t_s}{T_c}}$$

$$+ p_{R\frac{1}{2}} \sum_{k=0}^{\infty} a_k \sum_m \sum_{n'=0}^{M-1} \sum_{n=0}^{M-1} j^{n'-n} B_{m_0n} C_{mn'} \delta_{n-n'+(m_0-m)M+(k_0-k)\frac{t_s}{T_c}+\frac{1}{2}}$$

$$+ p_{R\frac{1}{2}} \sum_{k=0}^{\infty} a_k \sum_m \sum_{n'=0}^{M-1} \sum_{n=0}^{M-1} j^{n'-n} B_{m_0n} C_{mn'} \delta_{n-n'+(m_0-m)M+(k_0-k)\frac{t_s}{T_c}-\frac{1}{2}}$$

$$+ p_{R1} \sum_{k=0}^{\infty} a_k \sum_m \sum_{n'=0}^{M-1} \sum_{n=0}^{M-1} j^{n'-n} B_{m_0n} C_{mn'} \delta_{n-n'+(m_0-m)M+(k_0-k)\frac{t_s}{T_c}+1}$$

$$+ p_{R1} \sum_{k=0}^{\infty} a_k \sum_m \sum_{n'=0}^{M-1} \sum_{n=0}^{M-1} j^{n'-n} B_{m_0n} C_{mn'} \delta_{n-n'+(m_0-m)M+(k_0-k)\frac{t_s}{T_c}-1}$$

Observations:

- The first term is the principal contribution for each path, i.e., samples at the peak of the chip waveform.

[2] Although the correlator reference will be properly aligned to the signal, it is necessary to provide for mismatch of the reference and signal to later support 16-ary Orthogonal demodulation.

[3] Because of the linearity of filtering, the chip pulse is approximately symmetric.

[4] This is the Kronecker delta δ_{x0} with half-integer values of x allowed.

- The second two terms (having coefficients $p_{R½}$) are introduced when the multipath is sampled at half the chip time.

- The last two terms (coefficients p_{R1}) reflect the inter-chip effects of using, MSK or filtered PSK.

This may be further developed by specializing to multipath sampling at the chip time or half that value. In the following two equations, the expression in braces {} is a required constraint on remaining variables to be consistent with the original limits on the summation over n'. Note that in all cases this constraint has the form $\{0 \le n+\Delta \le M-1\}$.

For $\tau_s=T_c$

$$Y_{Bm_0} = \sum_{k=0}^{\infty} a_k \sum_m \sum_{n=0}^{M-1} j^{-(m_0-m)M-(k_0-k)} B_{m_0 n} C_{m,n+(m_0-m)M+(k_0-k)} \qquad \{0 \le n+(m_0-m)M+(k_0-k) \le M-1\}$$

$$+ p_{R1} \sum_{k=0}^{\infty} a_k \sum_m \sum_{n=0}^{M-1} j^{-(m_0-m)M-(k_0-k)-1} B_{m_0 n} C_{m,n+(m_0-m)M+(k_0-k)+1} \qquad \{0 \le n+(m_0-m)M+(k_0-k)+1 \le M-1\}$$

$$+ p_{R1} \sum_{k=0}^{\infty} a_k \sum_m \sum_{n=0}^{M-1} j^{-(m_0-m)M-(k_0-k)+1} B_{m_0 n} C_{m,n+(m_0-m)M+(k_0-k)-1} \qquad \{0 \le n+(m_0-m)M+(k_0-k)-1 \le M-1\}$$

For $\tau_s=\frac{1}{2}T_c$

$$Y_{Bm_0} = \sum_{\substack{k=0 \\ k-k_0 \text{ even}}}^{\infty} a_k \sum_m \sum_{n=0}^{M-1} j^{-(m_0-m)M-\frac{(k_0-k)}{2}} B_{m_0 n} C_{m,n+(m_0-m)M+\frac{(k_0-k)}{2}} \qquad \{0 \le n+(m_0-m)M+\frac{(k_0-k)}{2} \le M-1\}$$

$$+ p_{R\frac{1}{2}} \sum_{\substack{k=0 \\ k-k_0 \text{ odd}}}^{\infty} a_k \sum_m \sum_{n=0}^{M-1} j^{-(m_0-m)M-\frac{(k_0-k)+1}{2}} B_{m_0 n} C_{m,n+(m_0-m)M+\frac{(k_0-k)+1}{2}} \qquad \{0 \le n+(m_0-m)M+\frac{(k_0-k)+1}{2} \le M-1\}$$

$$+ p_{R\frac{1}{2}} \sum_{\substack{k=0 \\ k-k_0 \text{ odd}}}^{\infty} a_k \sum_m \sum_{n=0}^{M-1} j^{-(m_0-m)M-\frac{(k_0-k)-1}{2}} B_{m_0 n} C_{m,n+(m_0-m)M+\frac{(k_0-k)-1}{2}} \qquad \{0 \le n+(m_0-m)M+\frac{(k_0-k)-1}{2} \le M-1\}$$

$$+ p_{R1} \sum_{\substack{k=0 \\ k-k_0 \text{ even}}}^{\infty} a_k \sum_m \sum_{n=0}^{M-1} j^{-(m_0-m)M-\frac{(k_0-k)}{2}-1} B_{m_0 n} C_{mn+(m_0-m)M+\frac{(k_0-k)}{2}+1} \qquad \{0 \le n+(m_0-m)M+\frac{(k_0-k)}{2}+1 \le M-1\}$$

$$+ p_{R1} \sum_{\substack{k=0 \\ k-k_0 \text{ even}}}^{\infty} a_k \sum_m \sum_{n=0}^{M-1} j^{-(m_0-m)M-\frac{(k_0-k)}{2}+1} B_{m_0 n} C_{mn+(m_0-m)M+\frac{(k_0-k)}{2}-1} \qquad \{0 \le n+(m_0-m)M+\frac{(k_0-k)}{2}-1 \le M-1\}$$

We introduce the acyclic correlation function $R_{BC\Delta}$ as follows:

$$R_{B_m C_{m'} \Delta} = 0 \qquad \Delta \le -M$$

$$= j^{-\Delta} \sum_{n=-\Delta}^{M-1} B_{mn} C_{m',n+\Delta} \qquad -M < \Delta < 0$$

$$= j^{-\Delta} \sum_{n=0}^{M-1-\Delta} B_{mn} C_{m',n+\Delta} \qquad 0 \le \Delta < M$$

$$= 0 \qquad \Delta \ge M$$

This is a standard definition of the crosscorrelation of code sequences, except that the $j^{-\Delta}$ factor introduced by MSK signaling has also been absorbed into the definition.[5] With this, the above equations become

[5] This is convenient analytically, and it also means that the results can be used directly for PSK waveforms as well as for MSK.

For $\tau_s=T_c$

$$Y_{Bm_0} = \sum_{k=0}^{\infty} a_k \sum_m R_{B_{m_0}C_m,(m_0-m)M+(k_0-k)}$$
$$+ p_{R1} \sum_{k=0}^{\infty} a_k \sum_m R_{B_{m_0}C_m,(m_0-m)M+(k_0-k)+1}$$
$$+ p_{R1} \sum_{k=0}^{\infty} a_k \sum_m R_{B_{m_0}C_m,(m_0-m)M+(k_0-k)-1}$$

For $\tau_s=\frac{1}{2}T_c$

$$Y_{Bm_0} = \sum_{\substack{k=0 \\ k-k_0\ even}}^{\infty} a_k \sum_m R_{B_{m_0}C_m,(m_0-m)M+\frac{(k_0-k)}{2}}$$
$$+ p_{R\frac{1}{2}} \sum_{\substack{k=0 \\ k-k_0\ odd}}^{\infty} a_k \sum_m R_{B_{m_0}C_m,(m_0-m)M+\frac{(k_0-k)+1}{2}}$$
$$+ p_{R\frac{1}{2}} \sum_{\substack{k=0 \\ k-k_0\ odd}}^{\infty} a_k \sum_m R_{B_{m_0}C_m,(m_0-m)M+\frac{(k_0-k)-1}{2}}$$
$$+ p_{R1} \sum_{\substack{k=0 \\ k-k_0\ even}}^{\infty} a_k \sum_m R_{B_{m_0}C_m,(m_0-m)M+\frac{(k_0-k)}{2}+1}$$
$$+ p_{R1} \sum_{\substack{k=0 \\ k-k_0\ even}}^{\infty} a_k \sum_m R_{B_{m_0}C_m,(m_0-m)M+\frac{(k_0-k)}{2}-1}$$

These equations represent the outputs Y of correlators matched to reference codes B, due to input codes C at various multipath delays. It is necessary to further specialize these to consider signal demodulation and detection performance; this will be done in the next two sections.

The receiver filtering will be intentionally broadened relative to ideal matched filtering to avoid excessive inter-chip ISI (keep p_{R1} small); thus, the noise will be uncorrelated from sample to sample. The noise variances of correlator outputs is

$$\sigma_Y^2 = M\sigma_N^2 = 2MN_0B_N$$

When multiple correlator outputs are considered, the correlator noise is uncorrelated between correlators because the reference functions are orthogonal.

In the following sections, we shall focus on delay spreads greater than or equal to $2T_c$. This avoids considerable analytical complexity, since sampling at $\tau_s=T_c$ avoids handling correlations induced by sampling the multipath at half the chip rate. This restricts our attention to delay spreads ≥62.5 ns for the 32-Mchip/s modulation.

4 Demodulation Performance

4.1 Demodulation Mode Formulation

We begin with the expression for the correlator outputs specialized to the case of M-ary signaling, where the transmitted waveforms are $C_m = d_m P_m W_{K\,m}$ and the correlators are matched to $B_m = P_m W_K$. The correlator outputs for symbol m_0 are

$$Y_{P_{m_0}W_K} = \sum_{k=0}^{\infty} a_k \sum_m d_m R_{P_{m_0}W_K, P_m W_{K_m}, (m_0-m)M+(k_0-k)}$$

$$+ p_{R1} \sum_{k=0}^{\infty} a_k \sum_m d_m R_{P_{m_0}W_K, P_m W_{K_m}, (m_0-m)M+(k_0-k)+1}$$

$$+ p_{R1} \sum_{k=0}^{\infty} a_k \sum_m d_m R_{P_{m_0}W_K, P_m W_{K_m}, (m_0-m)M+(k_0-k)-1}$$

From here on we shall neglect the terms in p_{R1}. These reflect inter-chip effects due to bandwidth reduction, for example as encountered when PSK signals are filtered, and in any case for MSK-like signals. The value of p_{R1} is approximately .2; by contrast we must consider correlation side lobes of order .5 or higher relative to the autocorrelation peak, and multipath amplitudes which can be equal to the path being demodulated. Thus, the effects reflected by carrying the p_{R1} terms are of second-order in significance, and carrying them would complicate the analysis without benefit. The correlator outputs are

$$Y_{P_{m_0}W_K} = \sum_{k=0}^{\infty} a_k \sum_m d_m R_{P_{m_0}W_K, P_m W_{K_m}, (m_0-m)M+(k_0-k)}$$

We expect that symbol waveform m_0 can be significantly effected by the two immediately preceding symbols and the following symbol, for any multipath model. For 2 Msymbol/s signaling this is a span of 2 μs. Over this range of symbols we expand the sum

$$Y_{P_{m_0}W_K} = \sum_{k=0}^{\infty} a_k \Big[d_{m_0+1} R_{P_{m_0}W_K, P_{m_0+1}W_{K_{m_0+1}}, -M+(k_0-k)} + d_{m_0} R_{P_{m_0}W_K, P_m W_{K_m}, (k_0-k)}$$

$$+ d_{m_0-1} R_{P_{m_0}W_K, P_{m_0-1}W_{K_{m_0-1}}, M+(k_0-k)} + d_{m_0+2} R_{P_{m_0}W_K, P_{m_0-2}W_{K_{m_0-2}}, 2M+(k_0-k)} \Big]$$

In addition to the above signal components there is thermal noise. The correlator outputs are Rician-distributed with SNR

$$\gamma_K = \frac{\left|Y_{P_{m_0}W_K}\right|^2}{\sigma_Y^2} = \frac{\left|Y_{P_{m_0}W_K}\right|^2}{2MN_0B_N}$$

The probability of symbol error, conditioned on the specific waveforms $\mathbf{s} = \left\{P_{m_0+1}W_{K_{m_0+1}}, P_{m_0}W_{K_{m_0}}, P_{m_0-1}W_{K_{m_0-1}}, P_{m_0-2}W_{K_{m_0-2}}\right\}$ and the multipath profile $\mathbf{a} = \{a_0, a_0, a_0 \ldots\}$, is

$$P_e\big|_{\mathbf{s},\mathbf{a}} = 1 - \int_0^{\infty} dr_{K_{m_0}} \frac{r_{K_{m_0}}}{\sigma^2} e^{-\frac{r_{K_{m_0}}^2}{2\sigma^2} - \gamma_{K_{m_0}}} I_0\left(\frac{r_{K_{m_0}}}{\sigma^2}\sqrt{2\gamma_{K_{m_0}}}\right) \prod_{K \neq K_{m_0}} \left[\int_0^{r_{K_{m_0}}} dr_K \frac{r_K}{\sigma^2} e^{-\frac{r_K^2}{2\sigma^2} - \gamma_K} I_0\left(\frac{r_K}{\sigma^2}\sqrt{2\gamma_K}\right) \right]$$

In general it is necessary to average this probability of error over relevant distributions for **s** and **a**.

1.2 Gaussian channel

For the Gaussian channel we have $|\alpha_0|^2=1$ and (hence $k_0=0$) and $\alpha_k=0$ ($k>0$), so the signal component of the detection correlator outputs[6] are

$$Y_{P_{m_0}W_J} = a_0 R_{P_{m_0}W_J, P_{m_0}W_{K_{m_0}},0} = M a_0 \delta_{JK_{m_0}}$$

where δ_{nm} is the conventional Kronecker delta. These are the outputs of M correlators matched to the waveform set generated by combining the PN code used for the m^{th} symbol P_{m0} with each of the M Walsh functions W_J. The output[7] SNR is

$$\gamma = \frac{\left|Y_{P_{m_0}W_{K_{m_0}}}\right|^2}{\sigma_Y^2} = \frac{M^2|a_0|^2}{2MN_0B_N} = M\,SNR_{IN}$$

Most communications texts evaluate the error probability for M-ary OK[8] using the union bound

$$P_e(\gamma) \approx \frac{M-1}{2} e^{-\frac{\gamma}{2}}$$

An alternate estimate is obtained using a Padé-like approximation which preserves the correct behavior as $\gamma \to 0$.

$$P_e(\gamma) \approx \frac{M-1}{M + 2(e^{\frac{\gamma}{2}} - 1)}$$

The exact probability of error is given by

$$P_e = 1 - \int_0^\infty dr_1 \frac{r_1}{\sigma^2} e^{-\frac{r_1^2}{2\sigma^2} - \gamma} I_0\left(\frac{r_1}{\sigma^2}\sqrt{2\gamma}\right) \left[\int_0^{r_1} dr_2 \frac{r_2}{\sigma^2} e^{-\frac{r_2^2}{2\sigma^2}}\right]^{M-1}$$

where r_1 is the Rician variate of the correct correlator output and r_2 represents the Rayleigh variates of the M-1 incorrect correlator outputs. This has no closed-form solution, which is, of course, why the approximations are needed. Figure 1 compares numerical evaluation of the integrals to the approximations for M=16.

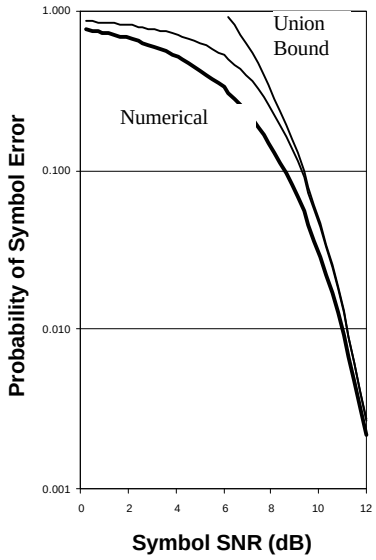

Figure 1 – P_e approximations

1.3 Diffuse Rayleigh Channel

Unlike the cases of Gaussian-channel demodulation and detection in general, it is not possible to procede on a purely analytical basis for demodulation of signals in the Rayleigh-channel case. This is due to the nonlinear interplay between multipath profiles and Walsh/PN coset cross-correlation side lobes in the symbol-decision process. We take the approach here of using simulation to construct the sufficient statistic derrived in 4.1 Demodulation Mode Formulation, then reverting to analytical techniques for subsequent evaluation. The key feature of this approach is minimization of the dimensionality to be handled via simulation. In particular, with noise as the only random element, simulation requires relatively long run times to produce meaningful results for

[6] α_0 still carries an unknown propagation phase.
[7] If a true matched filter were used, then this would be the familiar E/N_0.
[8] We shall evaluate the probability of symbol error based only upon the orthogonal-signaling component; in the absence of such errors, the error probability for the DBPSK component is completely negligible.

low probabilities of error. In the present case, the dimensionality of the random multipath is much larger than that of the thermal noise, and the signal waveforms themselves possess substantial dimensionality over which we must average. This makes simulation difficult. The approach used herein employs simulation to handle the averaging over many random selections of multipath profile and signal waveform, but uses standard analytical results via the union bound to handle thermal noise aspects without relying on simulation. This enables generation of a curve of symbol- or packet-error probability vs. SNR for the effort of averaging over signal and multipath parameters.

Rayleigh-distributed generation of random multpath envelopes was implemented by generating a discrete amplitude distribution having equal probabilities per amplitude bin, and whose amplitudes were derrived by averaging the amplitude over the amplitude bins according to the Rayleigh density. The results presented here employed 100 bins; re-running several of the cases using 1000 bins showned no difference. For each multipath component the amplitude was determined by selecting the amplitude bin using a uniform-distribution random number generator. The phase of each component was also generated as uniformly pseudorandom. These amplitude and phase components were used to obtain the real and imaginary components of the multipath samples.

Constaints imposed on the simulation by agreement among the 802.11 members were that the multipath samples must extend to 10 T_{RMS} and that multipath must be sampled at the finer of $T_{RMS}/2$ or T_c. When the multipath was sampled at sub-chip intervals, it was convolved with the receiver pulse (single-chip waveform) response at the same resolution, then subsequently decimated to the single-sample-per-chip sample rate used in receiver processing. This approach properly handles the continuous analog effects.

For each randomization there were generated a random complex multipath profile and a multi-symbol waveform with random data, and a single-symbol statistic was used to compute the probability of symbol error P_{SE} vs. SNR for a range of values as described in 6 Appendix: Error Probability Evaluation. The resulting curve must be considered a conditional P_{SE} vs. SNR, conditioned upon the specific multipath profile and signal waveform employed. The randomization was iterated for 4, 8 or 16 thousand cycles, and the curves vs. SNR averaged to arrive at the final curve of P_{SE} vs. SNR. The PER performance was calculated from these averaged probability of symbol error curves as also described in 6 Appendix: Error Probability Evaluation.

The following parameters were employed in simulations:

	Without Channel Matched Filter	With Channel Matched Filter
Multipath Extent	64 samples max.	128 samples max.
Signal Extent	64 chips = 4 symbols	128 chips = 8 symbols
Channel Matched Filter Span	N/A	8 chips = ½ symbol
Symbol Demodulated	3rd	6th

Longer spans for signal and multipath were used with the Channel Matched Filter because it tolerated larger T_{RMS}.

1.4 Performance

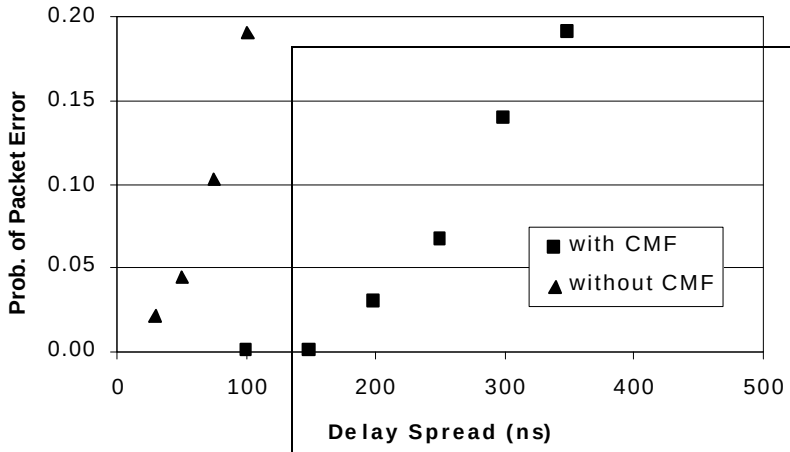

Figure 2 - PER vs. delay spread for noise-less case

Figure 2 shows the probability of packet error vs. delay spread for the noise-less case. The triangles indicate performance without a channel matched filter, while the rectangles indicate that with a channel matched filter. A 10% PER occurs at 275 ns delay spread using the channel matched filter. The increase in delay-spread tolerance from about 80 ns to 275 ns is dramatic enough to warrant including the CMF in the baseline proposal.

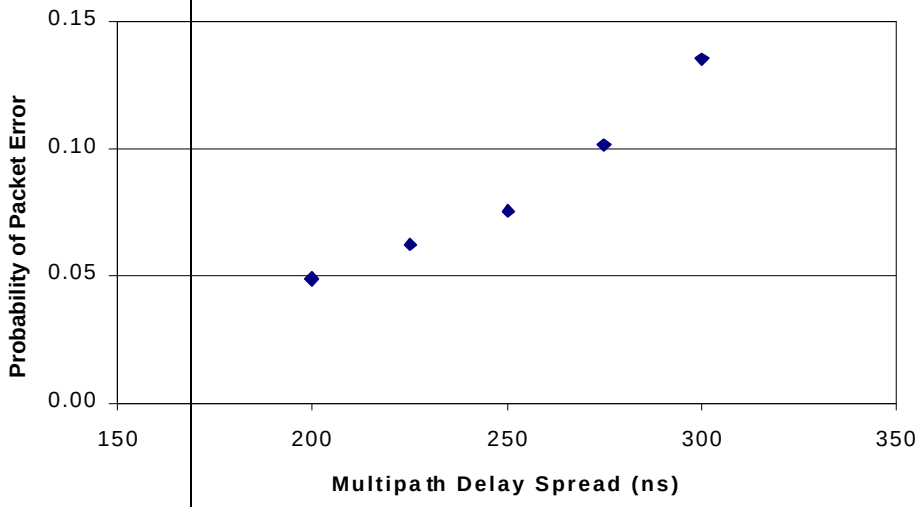

Figure 3 - Demodulation of 64-byte packet for noise-less case

As an independent check on the computation approach outlined above, a complete simulation was carried out, for thenoise-free case, in which 64-byte packets were fully demodulated for each random multipath profile. The results, shown in Figure 3, confirm the 10% PER at 275 ns. In addition, the full-frame simulation also enabled extraction of the conditional probability PCD described in 0. The value estimated for the symbol-error-based computation was 1/32=.03125. The value of PCD extracted from the full-frame

Figure 4

demodulation was .0283 at 275 ns and .0323 at 300 ns. Thus, the full-frame simulation and symbol-error-based computation are consistent.

Figures 4 and 5 present the probability of packet error vs. input SNR for a Rayleigh channel with 275 ns delay spread, and for a Gaussian channel.

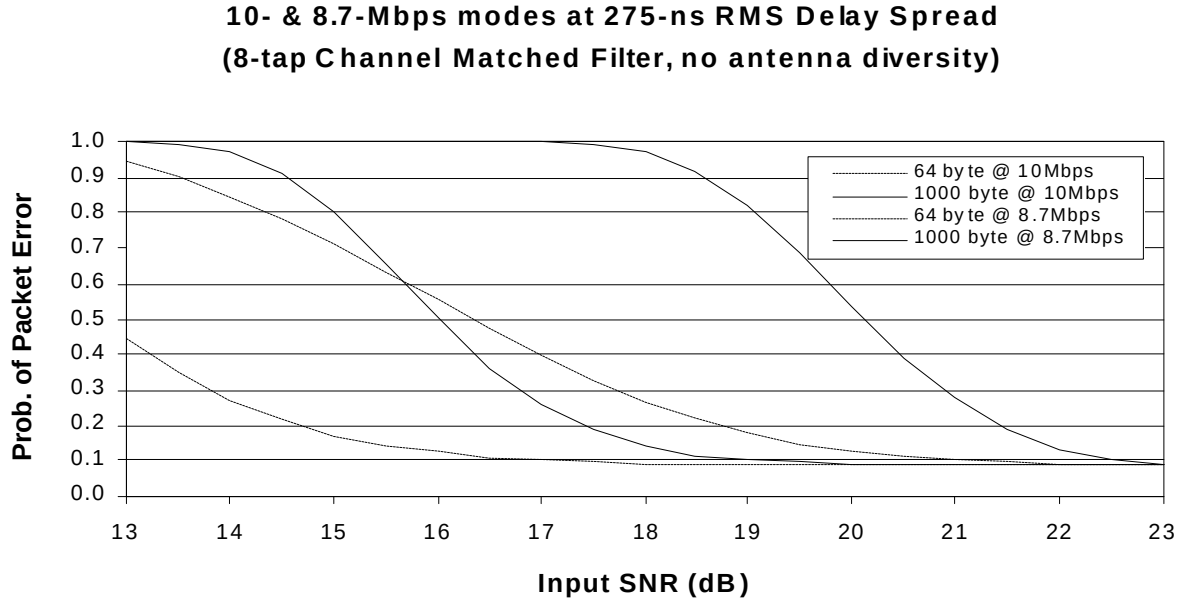

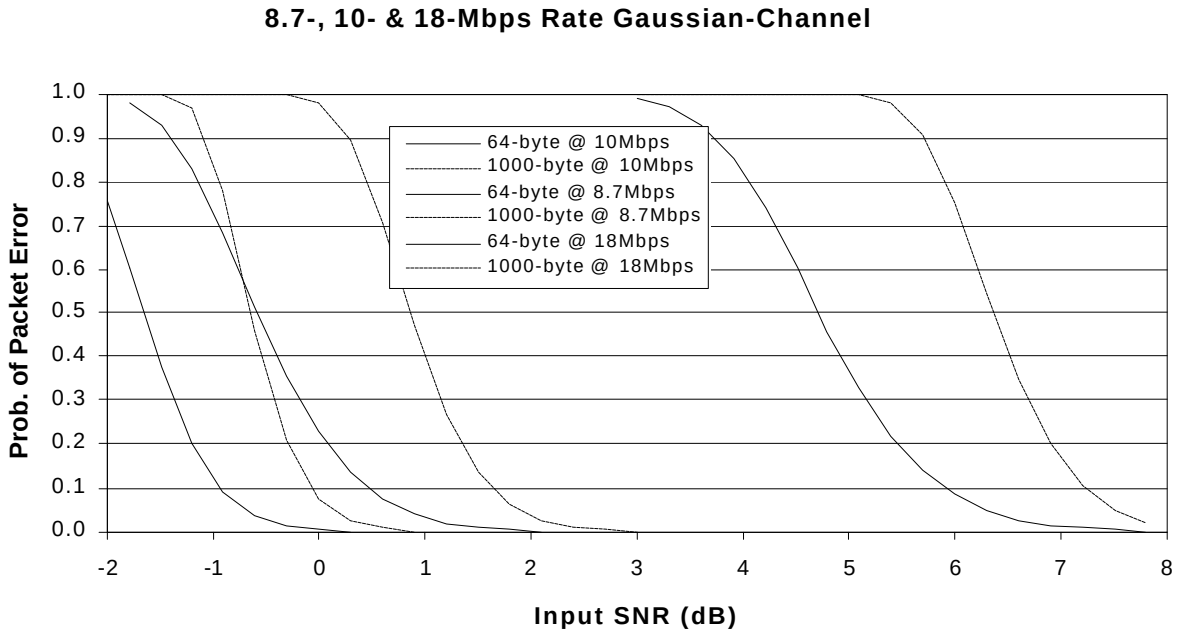
8.7-, 10- & 18-Mbps Rate Gaussian-Channel
Prob. of Packet Error
1.0
0.9
0.8
0.7
0.6
0.5
0.4
0.3
0.2
0.1
0.0
-2
-1
0
1
2
3
4
5
6
7
8
Input SNR (dB)
64-byte @ 10Mbps
1000-byte @ 10Mbps
64-byte @ 8.7Mbps
1000-byte @ 8.7Mbps
64-byte @ 18Mbps
1000-byte @ 18Mbps

Figure 5

2 Detection Performance

2.1 Acquisition Mode Formulation

The signal model was formulated to support analysis of 16-ary Noncoherent BiOrthogonal Keying (16-ary DBOK) with PN codes changing from symbol to symbol. In this section we specialize to the acquisition signal; i.e., a 16-chip code C_{Sn} repeated from symbol to symbol. The codes and their cyclic correlations are tabulated in section 5**Appendix: Sea**

$$\tilde{R}_{B_m C_{m'} \Delta} = j^{-\Delta} \sum_{n=0}^{M-1} B_{mn} C_{m', n+\Delta (\mathrm{mod} M)}$$

Consider the primary contribution (peak of chip waveform) to a correlator output Y_B for symbol m_0 due to a unit-amplitude signal component at delay $k\tau_s$

$$\begin{aligned} Y_B &= \sum_m R_{B_m C_{m'}, (m_0 - m)M + (k_0 - k)} \\ &= R_{B_m C_{m'}, (k_0 - k)} + R_{B_m C_{m'}, (M + k_0 - k)} \qquad k > k_0 \\ &= R_{B_m C_{m'}, (k_0 - k)} + R_{B_m C_{m'}, (-M + k_0 - k)} \qquad k < k_0 \\ &\equiv \tilde{R}_{B_m C_{m'}, (k_0 - k)} \end{aligned}$$

where we have recognized that the two acyclic correlations in each case actually make up the full cyclic correlation (using $j^M=1$). The correlator output, with the reference matched to and aligned with the signal at lag $k_0 T_c$, is

$$\begin{aligned} Y_B &= \sum_{k=0}^{\infty} a_k \tilde{R}_{SS, (k_0 - k)} \\ &+ p_{R1} \sum_{k=0}^{\infty} a_k \tilde{R}_{SS, (k_0 - k) + 1} \\ &+ p_{R1} \sum_{k=0}^{\infty} a_k \tilde{R}_{SS, (k_0 - k) - 1} \end{aligned}$$

During the search phase, the signal is repeated continually; the cyclic correlation function, in effect, aliases multipath components delayed by one or multiple symbols, whereas during demodulation these become intersymbol interference. We now explore this fold-over effect.

There are only MT_c possible sample times within the periodic symbol timing (assuming delay spread $\geq 2T_c$). Multipath at lag $(mM+n)T_c$ appears summed with multipath at lag nT_c, for all m. Because of this, we may re-cast the multipath description by summing multipath components separated by multiples of MT_c. For path models having strengths which are complex Gaussian, such a summation will also be complex Gaussian (Rayleigh amplitude). For example, the re-cast (cyclic) IDR channel impulse response is

$$\tilde{H}_c(t) = \sum_{k=0}^{M-1} \beta_k \delta (t - k t_s) \qquad t_s = T_c$$

where[10]

$$\sigma_{\beta k}^2 = \frac{\sigma_0^2 e^{-\frac{kT_c}{T_{RMS}}}}{1 - e^{-\frac{MT_c}{T_{RMS}}}}$$

[9] We use ~ (tilde) to distinguish cyclic correlations from acyclic.

[10] Note that the normalization is preserved, i.e., summing $\sigma^2_{\beta k}$ over the corresponding range of k.

2.2 Gaussian channel

For the Gaussian channel we have $|\alpha_0|^2=1$ and (hence $k_0=0$) and $\alpha_k=0$ ($k>0$), so the signal component of the detection correlator output[11] is

$$Y_B = \tilde{R}_{SS0} = M\mathsf{a}_0$$

and the output[12] SNR is

$$\mathsf{g} = \frac{|Y_B|^2}{\mathsf{s}_Y^2} = \frac{M^2|\mathsf{a}_0|^2}{2MN_0B_N} = M\,SNR_{\text{IN}}$$

The probability of detection vs. γ for a given probability of false alarm may be found as the non-fluctuating-target case in books on radar, e.g., DiFranco and Rubin,[13] although the reader is cautioned that radar texts generally use $R=2\gamma$ as the signal to noise, whereas communication texts use γ.

2.3 Diffuse Rayleigh Channel, T_{RMS}‡$2T_c$

Although the search correlator employs the same single-sample-per-chip computation as does the demodulation correlator, this is actually stepped along at half-chip intervals to limit the "straddling loss" to a fraction of a dB. During demodulation k_0 corresponds to the strongest multipath; during acquisition k_0 can be considered a hypothesis to be tested, i.e., whether the signal at delay $k_0\tau_s$ exceeds the threshold. Thus, we may compute the probability of detection as one minus the probability that correlator outputs for $k_0=0$ to M-1 all fall below the threshold. The correlator outputs for the k_0 are

$$Y_{Bk_0} = \sum_{k=0}^{M-1}\mathsf{b}_k\tilde{R}_{SS,(k_0-k)} + p_{R1}\sum_{k=0}^{M-1}\mathsf{b}_k\tilde{R}_{SS,(k_0-k)+1} + p_{R1}\sum_{k=0}^{M-1}\mathsf{b}_k\tilde{R}_{SS,(k_0-k)-1}$$

We ignore autocorrelation side lobes, assuming

$$\tilde{R}_{SS\Delta} = M\mathsf{d}_{0\Delta}$$

which results in

$$Y_{Bk_0} = \mathsf{b}_{k_0} + p_{R1}\mathsf{b}_{k_0+1} + p_{R1}\mathsf{b}_{k_0-1} \approx \mathsf{b}_{k_0}$$

To the same level of approximation, we can set $p_{R1}=0$ for detection since it is lower than expected autocorrelation side lobes. For a single-component Rayleigh-fluctuating signal the probability of detection vs. mean signal-to-noise ratio and probability of false alarm is given by[14]

$$P_d = P_{fa}^{1/(1+\bar{\mathsf{g}})}$$

Where γ is the mean SNR. For detection we test correlator amplitudes for M times of arrival, and the signal is missed only if detection fails on all M. For signal timing corresponding to k_0, the mean path SNR for the IDR channel is

$$\mathsf{g}_{k_0} = \frac{\overline{|Y_{Bk_0}|^2}}{\mathsf{s}_Y^2} = \frac{M^2\overline{|\mathsf{b}_{k_0}|^2}}{2MN_0B_N} = M2\mathsf{s}_{\mathsf{b}k_0}^2\,\overline{SNR}_{TOT}$$

The definition of $\overline{SNR}_{TOT}$ comes from

$$\sum_{k_0=0}^{M-1}\overline{|Y_{Bk_0}|^2} = \sum_{k_0=0}^{M-1}2\mathsf{s}_{\mathsf{b}k_0}^2 = \frac{2\mathsf{s}_0^2}{1-e^{-\frac{MT_c}{T_{RMS}}}}\sum_{k_0=0}^{M-1}e^{-\frac{kT_c}{T_{RMS}}} = \frac{2\mathsf{s}_0^2}{1-e^{-\frac{T_c}{T_{RMS}}}} = 1$$

---

[11] α_0 still carries an unknown propagation phase.
[12] If a true matched filter were used, then this would be the familiar E/N_0.
[13] DiFranco and Rubin, Radar Detection.
[14] Op Cit, DiFranco and Rubin.

independent of T_{RMS} for the IDR channel. Thus, the probability of detection in multipath is

$$P_d = 1 - \prod_{k_0=0}^{M-1} \left(1 - P_{fa}^{1/(1+M\,2\sigma^2_{bk_0}\,\overline{SNR})}\right)$$

2.4 Performance

Figure 6 shows the probability of missed detection vs. mean input SNR for the IDR channel, and vs. SNR for the Gaussian channel, for a detection criterion requiring threshold crossings on three successive symbols, at overall probability of false alarm of 10^{-6}. Requiring multiple threshold crossings enables improvement of detection performance, relative to single-symbol detection, without incurring the complexity of video combining before testing against a threshold. If we budget 1% of frame loss to missed detection, then it is clear from the figure that IDR multipath spreads from about 60 to 250 ns will incur 4- to 5-dB of fading loss, but that detectability improves monotonically with SNR.

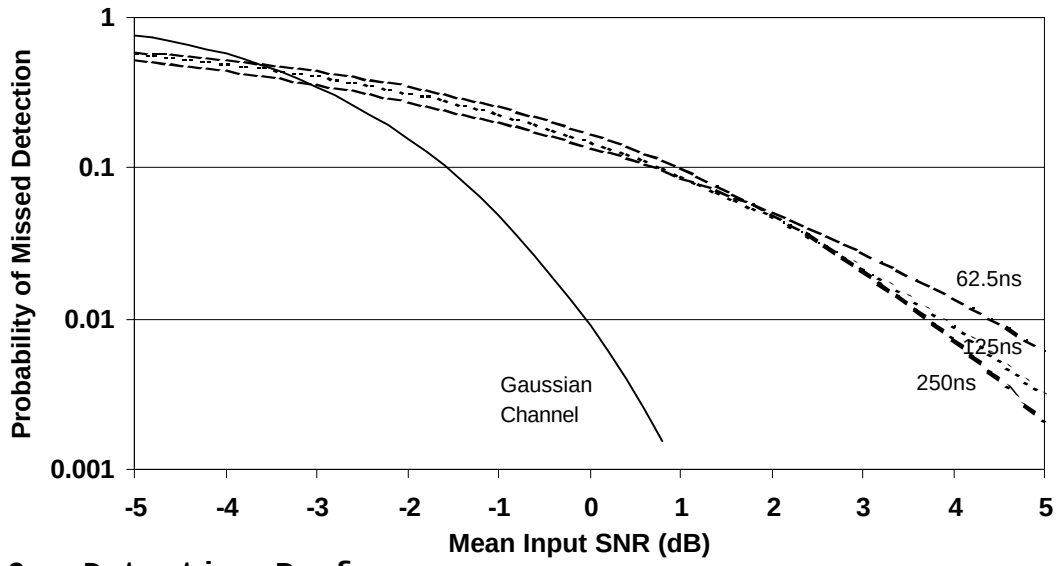

Figure 6 - Detection Performance

3 Interference Rejection

Previous sections assessed link performance in noise and multipath. This section considers interference rejection in the absence of multipath propagation effects.

3.1 Interference Rejection Formulation

From 1.2 **Gaussian channel** the signal response for the m[th] symbol is[15]

$$Y_{P_m W_J} = a_0 R_{PW_J, PW_{K_m}, 0} = M a_0 \delta_{JK_m}$$

where P_m is the PN code, J represents the Walsh-function correlator outputs and K_m the signal variant transmitted, respectively, α_0 is the signal strength and δ_{nm} is the Kronecker delta.

The baseband representation of the interfering signal is $x(t)e^{j2\pi\nu t}$, where x(t) is the envelope and ν is the offset frequency. It is assumed that the bandwidth of x(t) is small enough, and that ν is restricted to be sufficiently close to the signal carrier frequency, that no substantial roll-off due to receive filtering can be included in the processing gain calculation. The interference is sampled and applied to the correlator bank to produce

$$Y_{P_m W_J} = R_{PW_J, X} = \sum_{n=0}^{M-1} P_{mn} W_{Jn} x_n e^{j2\pi n \nu T_c}$$

We consider next the cases of narrowband CW interference and of band-limited Gaussian interference.

3.2 Narrowband CW Interference

We assume the interference to be $I e^{j2\pi\nu t}$, where I is the complex amplitude of the interference. The correlator outputs are

$$Y_{P_m W_J} = R_{PW_J, X} = I \sum_{n=0}^{M-1} P_{mn} W_{Jn} e^{j2\pi n \nu T_c}$$

As shown in document IEEE P802.11-97/116, for CW interference there is an abrupt drop to zero probability of error for some CW interference level when the largest possible interference output can no longer influence the data decision. We may determine this threshold by finding

[15] We have ignored here the p_{R1} terms as second-order.

$$Max\ over\ \{m, J\} \sum_{n=0}^{M-1} P_{mn} W_{Jn} e^{j2\pi n u T_c}$$

for the (M=16 bit) PN codes to be used. The 8 PN codes (coset leaders) have identical statistics in this regard. We show here the case of $P_{mn}=0158_H$. **Figure 7** shows $\left|Y_{P_m W_J}\right|^2$ (measured in dB relative to coherent response) vs. νT_c for all 16 correlator outputs. The worst-case situation occurs for ν within a symbol bandwidth of center frequency, where 2 correlator outputs produce outputs only 6-dB down from the coherent signal. As the CW interference level approaches the zero-error threshold, it is only the two channels having –6-dB responses for the interference which are of interest. When the signal would emerge from one of these two channel, which happens with probability 2/16, then it is possible for the CW interference to produce an amplitude out of an incorrect channel while simultaneously lowering the amplitude of the correct channel. This will occur when

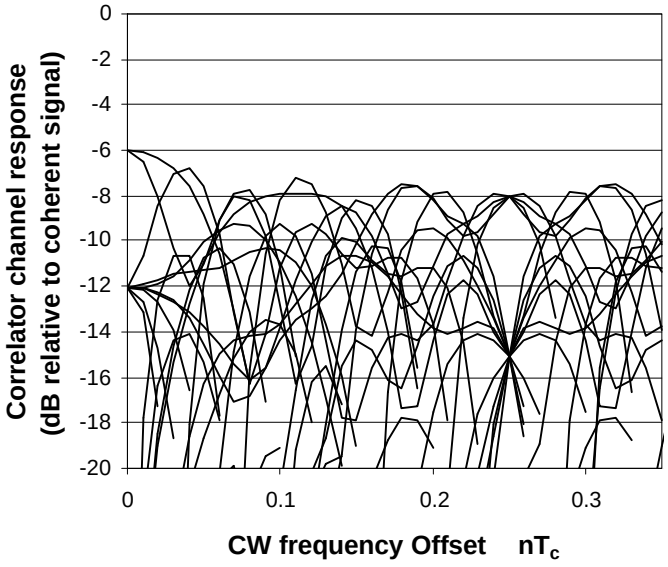

Figure 7 - Correlator output responses.

$$\left|\frac{I}{2}+a_0\right| \le \left|\frac{I}{2}\right|$$

Taking the arbitrary phase angle between the interference and signal to be Θ, an error occurs for

$$\left|\frac{I}{2a_0}+1\right| \le \left|\frac{I}{2a_0}\right| \quad \text{or} \quad 1+\frac{1}{4}\left|\frac{I}{a_0}\right|^2+\left|\frac{I}{a_0}\right|\cos(\Theta) \le \frac{1}{4}\left|\frac{I}{a_0}\right|^2$$

If a solution to this inequality exists, we may identify a boundary angle Θ_B between angles corresponding to making an error and angles for which no error occurs. The solution for this angle is

$$\cos(\Theta_B) = -\left|\frac{I}{a_0}\right|^{-1} = -\sqrt{\gamma} \quad \text{where} \quad \gamma \equiv \frac{|a_0|^2}{|I|^2}$$

is the signal-to-interference ratio. There clearly can be no error for γ>1; for γ<1 the solution for Θ_B is

$$\Theta_B = \pm\cos^{-1}(-\sqrt{\gamma})$$

The random phase Θ is distributed over 2π, so the probability of error is simply the fraction of 2π for which an error will occur times the 1/8 probability that the correct channel is one of the two channels under consideration, or

$$P_e(\gamma) = \frac{1}{8\pi}\cos^{-1}(\sqrt{\gamma})$$

It must be remembered that this is the asymptotic behavior near γ=1; for low signal-to-interference ratio the probability of error is larger than indicated by the above expression.

3.3 Narrowband Gaussian Interference

In this case we assume that x(t) is a Gaussian random variable. The correlator outputs due to noise are

$$Y_{P_m W_J} = \sum_{n=0}^{M-1} P_{mn} W_{Jn} x_n e^{j2\pi n u T_c}$$

It is assumed that the noise bandwidth is small enough, and that the frequency offset is confined, such that no substantial roll-off due to receive filtering is included as processing gain.

The processed interference remains Gaussian, since the correlation process is linear, so it remains only to find the mean-square correlator outputs.

$$\overline{\left|Y_{P_m W_J}\right|^2} = \overline{\sum_{n=0}^{15} P_{mn} W_{Jn} z_n \sum_{n'=0}^{15} P_{mn'} W_{Jn'} z_{n'}} = \sum_{n=0}^{15} \sum_{n'=0}^{15} P_{mn} W_{Jn} P_{mn'} W_{Jn'} \overline{z_n z_{n'}} = 2\sigma^2 \sum_{n=0}^{15} \sum_{n'=0}^{15} P_{mn} W_{Jn} P_{mn'} W_{Jn'} e^{-a|n-n'|T_c}$$

In the well-known case of white Gaussian noise, the correlator outputs are equal-variance, uncorrelated Gaussian variables. The above equation can be used to explore the effect of the bandwidth of the Gaussian interference. $P_m=0158_H$ was used, combined with the 16 Walsh functions, to calculate the correlator outputs shown in Figure 8.

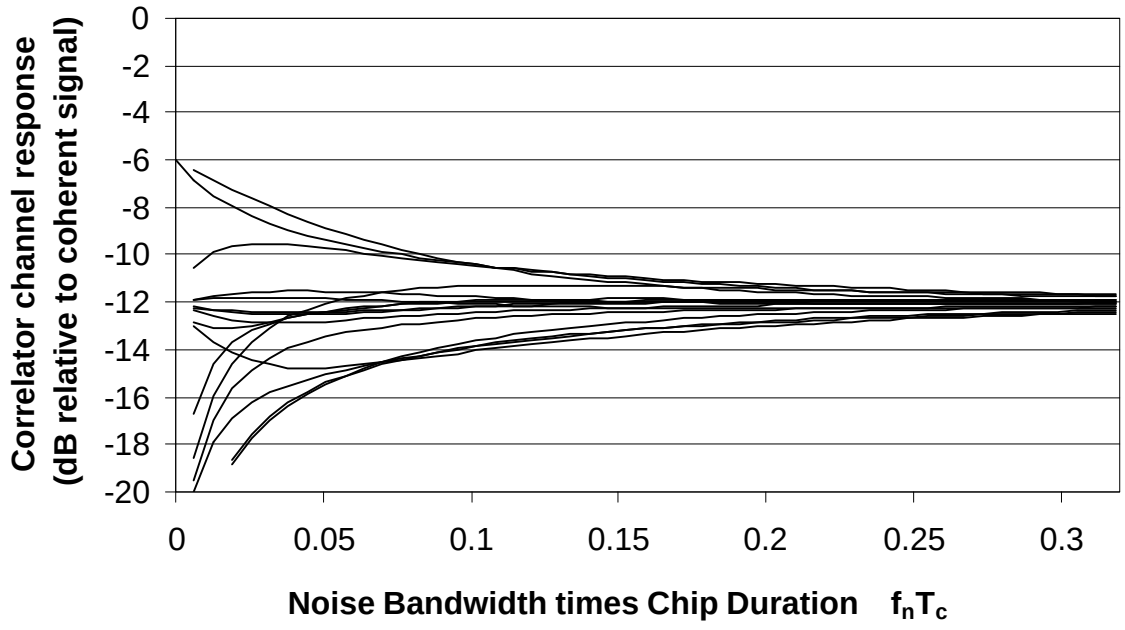

Figure 8 - Correlator output varainces, normalized to $2\sigma^2$, in dB relative to coherent response.

For very narrowband Gaussian interference ($a\rightarrow 0$) anomalous results are obtained. Two of the correlator outputs produce interference outputs suppressed only 6 dB relative to the coherent signal; this is due to lack of one-zero balance in the code for those correlator channels. On the other hand, six of the correlator outputs provide essentially infinite rejection of narrowband interference. The remaining eight outputs yield the same 12-dB suppression of narrowband interference as is the case for wideband interference.

Asymptotically ($a\rightarrow\infty$) all 16 correlator outputs produce the 12-dB suppression of the Gaussian interference expected from the 16 chips per symbol. It is clear that for noise bandwidths greater than approximately 25% of the chip rate (or 4 times the symbol rate) the processing gain is essentially the nominal 12 dB.

3.4 Performance

The S/I performance is summarized in Figure 9. CW interference produces a large error probability until the S/I approaches 0 dB, at which point the probability of error probability of error was estimated using the union boun having the smallest variance; that is, summing the binar individual channel responses to the interference. This v the chip rate (f_nT_c). Also shown is the asymptotic behav 20% noise bandwidth the performance is within a fraction of a dB of the asymptotic behavior for large noise bandwidth.

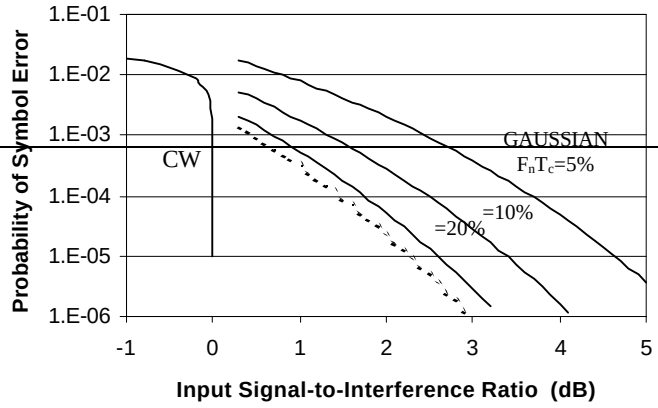

Figure 9 – Symbol error probability for CW and Gaussian interference

Interpreting this curve in terms of the "processing gain" test,[17] the dashed curve (decorrelated-noise limit) represents the 12-dB which is ten times $\log_{10}$ of the number of chips per symbol; CW interference would appear to have PG of 14 dB, while Gaussian noise at 10% and 5% would yield 10.9-dB and 9.7-dB, respectively.

[16] This ignores the receive filtering reduction on the noise, but this limit is simply for comparison.
[17] The implementation loss is assumed the same for all cases.

4 Appendix: Approximate MSK

The approximation to MSK to be implemented departs from an ideal, matched MSK system in the following:

a) the generation process combines a staircase approximation to a cosine pulse followed by a filter to offer an inexpensive implementation;

b) the transmit spectrum has lower side bands than ideal MSK;

c) the receive processor does not exactly match the chip waveform, preferring to keep the bandwidth somewhat higher for better multipath resolution.

The ideal MSK waveform has the baseband representation

$$s(t) = \sum_n j^n c_n p_{MSK}(t - nT_c)$$

where

T_c is the inverse of the chip frequency,
n is the chip index,
c_n is the chip value, and
$p_{MSK}(t)$ is the single-chip MSK waveform:

$$p_{MSK}(t) = \cos(\frac{\pi t}{2T_c}) \quad |t| < T_c$$
$$= 0 \qquad |t| < T_c$$

Ideal processing of the MSK waveform at the receiver begins with the (analog) chip matched filter[18] (CMF) for the MSK pulse.

$$p_{CMF}(t) = \frac{1}{T_c}\cos(\frac{\pi t}{2T_c}) \quad |t| < T_c$$
$$= 0 \qquad |t| < T_c$$

which results in the baseband waveform

$$w(t) = \sum_{k=0}^{\infty} a_k \sum_n j^n c_n R_{MSK}(t - kt_s - nT_c)$$

where the chip autocorrelation function is

$$R_{MSK}(t) = (1 - \frac{|t|}{2T_c})\cos(\frac{\pi t}{2T_c}) + \frac{1}{\pi}\sin(\frac{\pi t}{2T_c}) \qquad |t| < 2T_c$$
$$= 0 \qquad |t| > T_c$$

By contrast, the proposed implementation begins with a generator for the chip waveform which produces

$$p_G(t) = 1 \qquad |t| < .5T_c$$
$$= .37 \quad .5T_c < |t| < T_c$$
$$= 0 \qquad |t| > T_c$$

The transmit filtering is designed to minimize the energy taken out of the main spectral lobe while suppressing the side lobes. This may be accomplished using, e.g., 5th–order baseband filters plus some IF bandpass filter. As a result of this filtering, the generated pulse shape is replaced by the transmitter (equivalent-baseband) pulse shape $p_T(t)$, where

$$p_T(t) = p_G(t) * h_T(t)$$

[18] The filter's lack of causality is of no concern for present purposes.

so that the baseband representation of the transmitter waveform is

$$s(t) = \sum_n j^n c_n p_T(t - nT_c)$$

On receive, the waveform is passed through equivalent IF and baseband filtering. The resulting baseband complex signal is

$$s(t) = \sum_n j^n c_n p_R(t - nT_c)$$

where $p_R(t)$ is

$$p_R(t) = p_G(t) * h_T(t) * h_R(t)$$

Of significance is that the pulse shape of $P_R(t)$ is of considerably less time extent that would be the case for a true MSK pulse passed through an exact chip matched filter. Chip-to-chip amplitude overlap with this approach is typically less than .2, compared to .5 for true MSK. This is important for good multipath performance.

5 Appendix: Search Codes

The 16-bit codes selected for use during search and C_{Sn} are given in the following table, along with their cyclic autocorrelation functions, symmetric about the main lobe.

C_{Sn} (hex)	R_{ss0}	R_{ss1}	R_{ss2}	R_{ss3}	R_{ss4}	R_{ss5}	R_{ss6}	R_{ss7}	R_{ss8}
44BC	16	0	0	0	0	0	-4	0	-4
A0DC	16	0	0	0	0	0	-4	0	-4
D223	16	0	0	0	0	0	-4	0	-4
0A76	16	0	0	0	0	0	-4	0	-4
425C	16	0	0	0	0	4	0	-4	0
23A4	16	0	0	0	0	4	0	-4	0
245C	16	0	0	0	0	-4	0	4	0
A243	16	0	0	0	0	-4	0	4	0

These codes have excellent correlation properties for signal detection and selection of the strongest multipath component, having 4 or 5 zero values for autocorrelation side lobes nearest to the main lobe. When it is required to select codes for independent operation of BSAs, it is important to consider the peak and average cross-correlation values between the different codes (dB relative to main lobe) as shown below.

	44BC		A0DC		D223		0A76	
	Peak	rms	peak	Rms	Peak	rms	Peak	rms
44BC	0	-19.3	-2.5	-11.3	-6.0	-11.3	-6.0	-11.3
A0DC	-2.5	-11.3	0	-19.3	-6.0	-11.3	-6.0	-11.3
D223	-6.0	-11.3	-6.0	-11.3	0	-19.3	-2.5	-11.3
0A76	-6.0	-11.3	-6.0	-11.3	-2.5	-11.3	0	-19.3
425C	-4.1	-12.0	-8.5	-12.0	-4.1	-12.0	-4.1	-12.0
23A4	-4.1	-12.0	-4.1	-12.0	-4.1	-12.0	-8.5	-12.0
245C	-4.1	-12.0	-4.1	-12.0	-4.1	-12.0	-8.5	-12.0
A243	-4.1	-12.0	-8.5	-12.0	-4.1	-12.0	-4.1	-12.0

	425C		23A4		245C		A243	
	Peak	rms	peak	Rms	Peak	rms	Peak	rms
44BC	-4.1	-12.0	-4.1	-12.0	-4.1	-12.0	-4.1	-12.0
A0DC	-8.5	-12.0	-4.1	-12.0	-4.1	-12.0	-8.5	-12.0
D223	-4.1	-12.0	-4.1	-12.0	-4.1	-12.0	-4.1	-12.0
0A76	-4.1	-12.0	-8.5	-12.0	-8.5	-12.0	-4.1	-12.0
425C	0	-18.1	-6.0	-11.1	-6.0	-13.3	-6.0	-13.3
23A4	-6.0	-11.1	0	-18.1	-6.0	-13.3	-6.0	-13.3
245C	-6.0	-13.3	-6.0	-13.3	0	-18.1	-6.0	-11.1
A243	-6.0	-13.3	-6.0	-13.3	-6.0	-11.1	0	-18.1

6 Appendix: Error Probability Evaluation

6.1 Probability of Error Computation

The presence of multipath generally causes all correlator outputs to produce some signal component; Thus, the distribution of all outputs is Rician. The probability of error is

$$P_e = 1 - \int_0^\infty dr_{K_m} \frac{r_{K_m}}{\sigma^2} e^{-\frac{r_{K_m}^2}{2\sigma^2} - \gamma_{K_m}} I_0\left(\frac{r_{K_{m_0}}}{\sigma^2}\sqrt{2\gamma_{K_m}}\right) \prod_{K \neq K_m} \left[\int_0^{r_{K_{m_0}}} dr_K \frac{r_K}{\sigma^2} e^{-\frac{r_K^2}{2\sigma^2} - \gamma_K} I_0\left(\frac{r_K}{\sigma^2}\sqrt{2\gamma_K}\right) \right]$$

where K_m is the correct correlator channel. To evaluate this we make substitutions of the form $x = r / 2\sigma^2$.

$$P_e = 1 - \int_0^\infty du \; e^{-u-\gamma_{K_m}} I_0\left(\sqrt{4u\gamma_{K_m}}\right) \prod_{K \neq K_m} \left[\int_0^u dv_K \; e^{-v_K - \gamma_K} I_0\left(\sqrt{4v_K\gamma_K}\right) \right]$$

The union bound can be used for all situations in which the probability of error would be acceptable.

$$P_e = \sum_{K \neq K_m} \int_0^\infty du \; e^{-u-\gamma_{K_m}} I_0\left(\sqrt{4u\gamma_{K_m}}\right) \int_u^\infty dv_K \; e^{-v_K - \gamma_K} I_0\left(\sqrt{4v_K\gamma_K}\right)$$

6.2 Probability One Rician Variate Exceeds Another

We use the Marcum Q function to compute the binary probabilities[19] P_K, i.e., the probability that v_K exceeds u. If we define $a = \gamma_K$ and $b = \gamma_{K_m}$ then we have

$$P_K = \tfrac{1}{2}\left[1 - Q\left(\sqrt{b}, \sqrt{a}\right) + Q\left(\sqrt{a}, \sqrt{b}\right)\right]$$

For a=b this gives P_K=½. We assume from here on that b>a.[20]

$$P_K = \tfrac{1}{2}\left(\frac{b-a}{b+a}\right) \int_{\frac{b+a}{2}}^\infty e^{-u} I_0\left(\frac{2u\sqrt{ba}}{b+a}\right) du \qquad b > a$$

If a=0 we have the familiiar result that $P_K = \frac{1}{2} e^{-b/2}$. More generally, we substitute the series $\sum_{n=0}^\infty \frac{1}{(n!)^2}\left(\frac{x}{2}\right)^{2n}$ for $I_0(x)$

$$P_K = \tfrac{1}{2}\left(\frac{b-a}{b+a}\right) \sum_{n=0}^\infty \frac{\left(\frac{ba}{(b+a)^2}\right)^n}{(n!)^2} \int_{\frac{b+a}{2}}^\infty u^{2n} e^{-u} du$$ and carry out the integral

$$P_K = \tfrac{1}{2}\left(\frac{b-a}{b+a}\right) e^{-\frac{b+a}{2}} \sum_{n=0}^\infty \frac{(2n)!}{(n!)^2}\left(\frac{ba}{(b+a)^2}\right)^n \sum_{m=0}^{2n} \frac{1}{m!}\left(\frac{b+a}{2}\right)^m$$

[19] M. Schwartz, W. R. Bennett and S. Stein, Communications Systems and Techniques. New York: McGraw-Hill, 1966, pp. 585-587.

[20] If b<a, then we interchange the roles of a and b and complement the resulting computed probability to find P_K.

This form can be recursively computed, as can be seen by defining K=ba/(b+a) and C=(b+a)/2.

$$P_K = \frac{b-a}{2(b+a)} e^{-\frac{b+a}{2}} \sum_{n=0}^{\infty} \frac{(2n)!}{(n!)^2} K^n \sum_{m=0}^{2n} \frac{1}{m!} C^m$$

If we let S_N be the sum over n carried to N terms, and H_N be the sum over m carried to 2_N terms

$$S_N = \sum_{n=0}^{\infty} \frac{(2n)!}{(n!)^2} K^n \sum_{m=0}^{2n} \frac{1}{m!} C^m = S_{N-1}$$

$$+ \frac{2(2N-1)}{N} KK^{N-1} \left(H_{N-1} + \frac{(C^2 + 2NC)C^{2(N-1)}}{(2N)!} \right)$$

For each n the series over m is carried to completion, so it is not a source of error. Since the series in n has the variable $ba/(b+a)^2$ raised to the n^{th} power, and since this variable is never larger than .25, we expect that the series in n can be readily truncated without large error. Unfortunately, the sum over m is approaching exp[(b+a)/2] for large n, and this results in overflow problems for the inner summation as well as underflow in the exponential. The recursion for b+a small uses the equations directly, while that for b+a large associates the exponential with the sum over m and employs logarithms.

We now have a robust algorithm for computing the probability of error when both variates are Rician for all values of a and b.

6.2.1 For use when b+a is small

Define: C=(b+a)/2
K=b*a/(b+a)^2
F=.5*(b-a)/(b+a)

Init: S=1,G=1,H=1,TNF=1,C2N=1

Recursion in N:
TNF=TNF*N*(4*N-2)
G=G*K(4*N-2)/N
H=H+C2N*C*(2*N+C)/TNF
C2N=C2N*C^2
D=G*H
S=S+D

Terminate recursion: D/S<ε

Result: P=EXP(-C)*F*S

6.2.2 For use when b+a is large

Define: C=(b+a)/2
K=b*a/(b+a)^2
F=.5*(b-a)/(b+a)
LC=Ln(C)
LK=Ln(K)

Init: LS=0,LG=0,LH=0,LTNF=0,LC2N=0

Recursion in N:
LTNF=LTNF +Ln(2*N*(2*N-1))
LG=LG+LK+Ln((4*N-2)/N)
LQ=LC2N+LC+Ln(2*N+C)-LTNF
H=H+Ln(1+Exp(LQ))
LC2N=LC2N+2*LC
LD=LG+LH
LS=LS+Ln(1+Exp(LD-LS)

Terminate recursion: LD-LS<Ln(ε)

Result: P=F*Exp(S-C)

6.3 Probability One Gaussian Variate Exceeds Another in Magnitude

In the case of coherent reception, a similar formulation may be used and this section applies to the computation of symbol-error probability. Assume $\bar{x} = \sqrt{2\sigma^2\gamma_x} > \bar{y} = \sqrt{2\sigma^2\gamma_y} > 0$; if the the means are reversed[21], then interchange the roles of x and y, and complement the probability. In order to compute the probability correctly we must sum probabilities of mutually exclusive events.

	$P(x>0) = 1-\frac{1}{2}erfc\left(\sqrt{\gamma_x}\right)$	$P(x<0) = \frac{1}{2}erfc\left(\sqrt{\gamma_x}\right)$
$P(y>0) = 1-\frac{1}{2}erfc\left(\sqrt{\gamma_y}\right)$	$P(y>x) = \frac{1}{2}erfc\left(\sqrt{\frac{\gamma_x}{2}} - \sqrt{\frac{\gamma_x}{2}}\right)$	$P(y>-x) = 1-\frac{1}{2}erfc\left(\sqrt{\frac{\gamma_x}{2}} + \sqrt{\frac{\gamma_x}{2}}\right)$
$P(y<0) = \frac{1}{2}erfc\left(\sqrt{\gamma_y}\right)$	$P(y<-x) = \frac{1}{2}erfc\left(\sqrt{\frac{\gamma_x}{2}} + \sqrt{\frac{\gamma_x}{2}}\right)$	$P(y<x) = 1-\frac{1}{2}erfc\left(\sqrt{\frac{\gamma_x}{2}} - \sqrt{\frac{\gamma_x}{2}}\right)$

Here we have used directly the well-know results for making correct sign decisions. The relative-magnitude probabilities recognize the sum/difference of the means as well as the corresponding doubling of the noise variance. The probability is

$$P(|y|>|x|) = \left(1-\tfrac{1}{2}erfc\left(\sqrt{\gamma_x}\right)\right)\left(1-\tfrac{1}{2}erfc\left(\sqrt{\gamma_y}\right)\right)\left(\tfrac{1}{2}erfc\left(\sqrt{\frac{\gamma_x}{2}} - \sqrt{\frac{\gamma_y}{2}}\right)\right)$$
$$+\left(\tfrac{1}{2}erfc\left(\sqrt{\gamma_x}\right)\right)\left(1-\tfrac{1}{2}erfc\left(\sqrt{\gamma_y}\right)\right)\left(1-\tfrac{1}{2}erfc\left(\sqrt{\frac{\gamma_x}{2}} + \sqrt{\frac{\gamma_y}{2}}\right)\right)$$
$$+\left(1-\tfrac{1}{2}erfc\left(\sqrt{\gamma_x}\right)\right)\left(\tfrac{1}{2}erfc\left(\sqrt{\gamma_y}\right)\right)\left(\tfrac{1}{2}erfc\left(\sqrt{\frac{\gamma_x}{2}} + \sqrt{\frac{\gamma_y}{2}}\right)\right)$$
$$+\left(\tfrac{1}{2}erfc\left(\sqrt{\gamma_x}\right)\right)\left(\tfrac{1}{2}erfc\left(\sqrt{\gamma_y}\right)\right)\left(1-\tfrac{1}{2}erfc\left(\sqrt{\frac{\gamma_x}{2}} - \sqrt{\frac{\gamma_y}{2}}\right)\right)$$

This can be evaluated for the Gaussian-channel limit

$$P(|y|>|x|) = \frac{1}{2}\left[erfc\left(\sqrt{\frac{\gamma_x}{2}}\right)\left(1-\tfrac{1}{2}erfc\left(\sqrt{\gamma_x}\right)\right) + erfc\left(\sqrt{\gamma_x}\right)\left(1-\tfrac{1}{2}erfc\left(\sqrt{\frac{\gamma_x}{2}}\right)\right)\right]$$

[21] There is no loss in generality in assuming that the means are positive.

6.4 Probability of Packet Failure

The probability of symbol error results from the statistical average over the distributions for the thermal noise, for the data and spreading codes, and for the multipath. There are three situations to consider:

Noise Only: In this case the random distribution is that of the thermal noise; for a given SNR the symbol errors are independent from symbol to symbol, with probability P_{eN}. The probability that packet having N_s symbols will fail is

$$P_F = 1-(1-P_{eN})^{N_s}$$

Multipath Only: In this case the random distributions are those of the multipath and code/data combination; the SNR is infinite, and the residual probability of symbol error P_{eI} is the product of the probability P_{CB} that the multipath profile is one which causes errors in the absence of noise and the probability P_{CD} that the code and data combination are sensitive to this bad channel condition. However, when this happens, the symbol errors are highly correlated throughout the packet because the multipath is static over a packet. For 16-bit codes[22] we assume that the conditional probability of error, given a bad channel condition, is P_{CD}=1/8, for some coset. However, since there are four cosets used to form any code channel, and since it is likely that only one of the cosets is disturbed by a particular "bad" multipath profile, the correct value for calculations is P_{CD}=1/32. The probability that packet having N_s symbols will fail is

$$P_F = (1-(1-P_{CD})^{N_s})P_{CB}$$

Multipath and Noise: In this case the random distributions of both the noise and multipath must be accommodated. When the SNR is very high the multipath-only behavior must be exhibited, while the noise-only behavior should dominate when $P_e >> P_{eI}$. We seek a procedure for calculating P_F consistent with the above, and which may be applied to computations without requiring a decision as to the dominant behavior (i.e., multipath or noise). We may separate the probability of symbol error into mutually exclusive good- and bad-channel cases, then employ the appropriate probability of packet failure. The packet-failure probability is then

$$P_F = \left(1-(1-P_{en})^{N_s}\right)(1-P_{CB}) + (1-(1-P_{CD})^{N_s}(1-P_{en})^{N_s})P_{CB}$$

The non-thermal error probability must be subtracted from P_e, and that $P_{CD}=1/8P_{eI}$ can be substituted, to yield

$$P_F = \left(1-(1-P_{en}+P_{eI})^{N_s}\right)(1-32P_{eI}) + (1-(\tfrac{31}{32})^{N_s}(1-P_{en}+P_{eI})^{N_s})32P_{eI}$$

6.5 Noise Re-Normalization for Channel Matched Filter

The performance computation used is a hybrid between simulation and analytical techniques. The channel impulse response, data and spreading codes are repeatedly selected simulation-style from a large space in order to generate possible received waveforms. However, because simulation is particularly inefficient in computing low probabilities of symbol error, this is done using the signal amplitudes and analytical expressions for the probability of symbol error vs. SNR. The insertion of a channel matched filter (CMF) causes some difficulty for the hybrid calculation, as opposed to simulation, because the noise is re-normalized in the process.

6.5.1 Standard Receiver

A "largest-of" receiver correlates against the possible received waveforms, then selects as the correct hypothesis that which produces the largest magnitude for the correlation. In a white-noise environment the signal components are

[22] This was shown in document 97-120 for a specific code being used as an example; since the codes are statistically similar, it is reasonable to use this value for our calculations.

$$S_m = A\sum_{n=0}^{N_c-1} C_{mn}C_{m'n}$$

where A is the unknown complex amplitude, N_c is the number of chips, C_{mn} is the code pattern and m' corresponds to the data (i.e., the actual waveform transmitted). The noise variance is

$$N_m^2 = \overline{\left|\sum_{n=0}^{N_c-1} z_n C_{mn}\right|^2} = \sum_{n'}^{N_c-1}\sum_{n=0}^{N_c-1} \overline{z_{n'}z_n} C_{mn'}C_{mn} = 2\sigma^2 \sum_{n}^{N_c-1} C_{mn}^2$$

which is the same for all channels. The SNR is found by using the magnitude squared of the output for the correct channel

$$\frac{|S_{m'}|^2}{N_{m'}^2} = \frac{\left|A\sum_{n=0}^{N_c-1} C_{mn}C_{m'n}\right|^2}{2\sigma^2\sum_{n}^{N_c-1} C_{mn}^2} = \frac{|A|^2}{2\sigma^2}\frac{N_c^2}{N_c} = N_c\frac{|A|^2}{2\sigma^2}$$

Since the noise is added at the receiver, while the signal is convolved with the channel impulse response before entering the receiver, the probability of symbol error can be computed using the standard expressions by simply computing the magnitudes of the correlator outputs. The noise is unaffected in this process. Of course, the channel distortions generally cause the SNR in the incorrect channels to be non-zero, but this is handled using the union bound with pair-wise error probabilities for two Rician variates.

6.5.2 Receiver with CMF

The form of the above SNR makes clear the difficulty incurred when a CMF is inserted. Unlike the previous case, which left the noise unaltered, the presence of a CMF inside the receiver means that the noise is affected. Thus, the denominator of the SNR expression must be changed. The cascade of the CMF and the correlators must be considered as the overall linear processing reference function. Thus, we define

$$g_{mn} = C_{mn} * d_n = \sum_{n'=\{0,n-N_t\}}^{\min\{n,N_c-1\}} C_{mn'}d_{n-n'}$$

where d_n is the impulse response of the CMF (assumed not to perfectly match) and N_t is the number of filter taps. The received waveform is $r_{mn} = C_{m'n} * c_n$ where c_n is the true channel impulse response. With this definition we may write the SNR

$$\frac{|S_{m'}|^2}{N_{m'}^2} = \frac{|A|^2}{2\sigma^2}\frac{\left|\sum_{n=0}^{N_c+N_t-1} r_{mn}g_{m'n}^*\right|^2}{\sum_{n}^{N_c+N_t-1}|g_{m'n}|^2}$$

We use the previous formulation (i.e., union bound with pair-wise error probabilities) with the SNR per correlator output replaced by the above ratio of summations. However, note that the noise component now varies for each channel; this is inconsistent with the dual-Rician error formulation used, which assumes equal variances. A reasonable approximation can be used to avoid a considerably more complex formulation: we shall compute the noise variance summation as statistically averaged over random codes, then use this single variance for all channels. This will take the noise re-normalization into account in a reasonable manner. We write the noise summation

$$\sum_n |g_{m'n}|^2 = \sum_n \sum_{n'} \sum_{n''} C_{mn'}C_{mn''}d_{n-n'}d_{n-n''}^*$$

We use the average over all codes by asserting that $\overline{C_{mn'}C_{mn''}} = \delta_{n'n''}$ which leads to

$$\overline{\sum_n |g_{m'n}|^2} = \sum_n \sum_{n'} \sum_{n''} \delta_{n'n''}d_{n-n'}d_{n-n''}^* = \sum_n \sum_{n'} |d_{n-n'}|^2 = N_c\sum_{n'} |d_n|^2$$

This result requires careful consideration of the limits of the summations. A simple approach to handling the noise re-normalization is to require $\sum_{n'} |d_n|^2 = 1$ which avoids any required change in original computation procedure.